Research Article

For reprint orders, please contact: reprints@futuremedicine.com

Nanomedicine

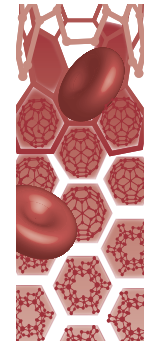

Are they in or out? The elusive interaction between Qtracker®800 vascular labels and brain endothelial cells

Aim: Qtracker®800 Vascular labels (Qtracker®800) are promising biomedical tools for high-resolution vasculature imaging; their effects on mouse and human endothelia, however, are still unknown. **Materials & methods:** Qtracker®800 were injected in Balb/c mice, and brain endothelium uptake was investigated by transmission electron microscopy 3-h post injection. We then investigated, *in vitro*, the effects of Qtracker®800 exposure on mouse and human endothelial cells by calcium imaging. **Results:** Transmission electron microscopy images showed nanoparticle accumulation in mouse brain endothelia. A subset of mouse and human endothelial cells generated intracellular calcium transients in response to Qtracker®800. **Conclusion:** Qtracker®800 nanoparticles elicit endothelial functional responses, which prompts biomedical safety evaluations and may bias the interpretation of experimental studies involving vascular imaging.

Keywords: calcium imaging • cytosolic calcium transients • human umbilical vein endothelial cells • mouse brain endothelium • nanoparticles • nanoparticle uptake • transmission electron microscopy

Beatrice Mihaela Radu[1,2], Mihai Radu*[,1,3], Cristina Tognoli[1], Donatella Benati[1], Flavia Merigo[1], Michael Assfalg[4], Erika Solani[5], Chiara Stranieri[5], Alberto Ceccon[4], Anna Maria Fratta Pasini[5], Luciano Cominacini[5], Placido Bramanti[6], Francesco Osculati[1,6], Giuseppe Bertini[‡,1] & Paolo Francesco Fabene[‡,1]

[1]Section of Anatomy & Histology, Department of Neurological & Movement Sciences, University of Verona, Verona 37134, Italy

[2]Department of Anatomy, Animal Physiology & Biophysics, Faculty of Biology, University of Bucharest, Bucharest 050095, Romania

[3]Department of Life & Environmental Physics, 'Horia Hulubei' National Institute for Physics & Nuclear Engineering, Magurele 077125, Romania

[4]Department of Biotechnology, University of Verona, Verona 37134, Italy

[5]Section of Internal Medicine, Department of Medicine, University of Verona, Verona 37134, Italy

[6]IRCCS Centro Neurolesi 'Bonino Pulejo', Messina, Italy

*Author for correspondence:
Tel.: +39 0458027670
Fax: +39 0458027163
mihai.radu@univr.it

[‡]Authors contributed equally

Cerebral vasculature imaging is required in the diagnosis of cerebrovascular pathology and healthcare stakeholders are increasingly interested in safer, cheaper and higher resolution clinical imaging solutions. In the last decade, the field of nanotechnology has exploded, and new nanomedicine and nanoneuromedicine approaches have been proposed as alternative or complementary solutions to already existing vasculature imaging tools (e.g., MRI- and/or CT-based angiography).

Several metallic and organic nanomaterials have been approved by the US FDA at different clinical trial stages as diagnostic tools; semiconductor nanomaterials (for example, quantum dots) are, on the other hand, generally considered for research use only [1,2]. Recently, a new generation of fluorescent silica nanoparticles called Cornell dots (C-dots), with efficient urinary excretion [3] and effective cancer-targeting properties [4,5], received FDA approval for clinical use. This FDA approval opens a new era for nanomedicine, and deeper understanding of cell-specific action of semiconductor-based nanoparticles is urgently needed.

Rapid nanotechnology advances in preclinical brain vasculature imaging [6–10] have substantially increased our ability to unveil vascular contributions to the pathogenesis of brain ischemia, brain tumor formation, Alzheimer disease and epilepsy [11–13].

Quantum-dot nanoparticles (QDs) gained popularity over the last decade [14], due to their superior optical properties with respect to conventional organic dyes [15–17]. In particular, Qtracker® vascular labels (Qtracker®565, Qtracker®605, Qtracker®655, Qtracker®705 and Qtracker®800, named according to their emission wavelength) have been designed for *in vivo* deep-tissue imaging of blood vessel distribution and morphological properties in small animals [18]. The high-wavelength Qtracker®800 allows the deepest imaging of tissue vasculature of the series. Preclinical *in vivo* imaging studies of the vessels using Qtracker®800 have already been carried out

Future Medicine part of fsg

to highlight mouse tumor vascularization [19] and bone marrow vasculature [20].

Biocompatibility is a key requirement for QD-based *in vivo* vascular imaging. The 'ideal' QDs should be 'inert' with respect to the microenvironment (e.g., circulating and endothelial cells). In practice, this desired property is usually sought by coating the QDs with a thin polymer layer, one of the most used being PEG, without any functional group. This layer reduces the nonspecific interaction of coated QDs with the surrounding molecular species, including those present on the cell plasma membrane [18,21]. Indeed, PEG coating of QDs drastically minimizes nonspecific interactions [18] and decreases cellular uptake rate, as proved in three tumor cell lines [22].

A very recent report, however, demonstrated the uptake of PEG-coated silica nanoparticles in brain endothelial cells [23]. Since these coated nanoparticles are between 25 and 100 nm (i.e., almost five- to ten-times the core diameter of QDs) and given the authors' claim that nanoparticle transport across the blood–brain barrier is size-dependent, we wondered whether PEG-coated QDs might show significant interactions with endothelial cells. To our knowledge, there are no published reports describing such direct interaction.

Based on these premises, we investigated: whether *in vivo* Qtracker®800 are uptaken by endothelial cells, and the functional consequences of endothelial exposure to Qtracker®800, studied *in vitro*. First, the hydrodynamic diameter of Qtracker®800 was estimated by dynamic light scattering (DLS) and the core size was calculated from electron microscopy images in order to characterize the nanoparticles. Next, in a set of *in vivo* experiments, Qtracker®800 uptake in mouse brain endothelia was investigated by electron microscopy. As previously described, many aspects of vascular endothelium physiology are regulated by calcium signaling pathways, since most of the stimuli relaxing or contracting brain capillaries act directly on the endothelial cells, producing changes in intracellular-free calcium concentration [24–26]. Based on the above, we also investigated *in vitro* the ability of a Qtracker®800 flux to induce fluctuations of free cytosolic calcium concentration and/or changes in mouse brain endothelial cell viability. We have also extended our *in vitro* study to another type of endothelial cells (human umbilical vein endothelial cells [HUVECs]) in order to discriminate between a specific effect on mouse brain endothelial cells and an ubiquitous effect.

Materials & methods

Chemicals

Qtracker®800 (Q21071MP, lot #1216103, Life technologies, NY, USA) were dissolved in 0.9% saline solution for the *in vivo* studies, and in Ringer HEPES-buffered solution (NaCl: 140 mM; KCl: 5.6 mM; $MgCl_2$: 2 mM; $CaCl_2$: 2 mM; glucose: 10 mM; HEPES 10 mM; pH 7.4 with NaOH) or phosphate-buffered solution (5 mM; pH 7.4) for the *in vitro* experiments. Fura-2 acetoxymethyl ester (Fura-2 AM) and pluronic acid F-127 (Life technologies) were dissolved in Ringer solution. All other reagents were purchased from Sigma-Aldrich (MO, USA).

Hydrodynamic size measurements by DLS

DLS was performed on Qtracker®800 using a Zetasizer Nano ZS instrument (Malvern Instruments Ltd, MA, USA) operating with a 633 nm He-Ne laser light source and a fixed detector angle of 173°, as previously described [27]. Qtracker®800, 2-µM stock solution of 2 µM in 50 mM borate buffer, pH 8.3 (Life Technologies) was diluted to the range of 40–80 nM either in Ringer solution or in saline solution (See section Chemicals). Lower particle concentrations resulted in poor signal/noise and large fit errors (using either single or multiple exponential models). Hydrodynamic diameter values were determined by averaging the intensity-weighted size distributions obtained from 20 successive DLS runs of 10 s each. Measurements were repeated three-times and results are reported as mean ± standard deviation (SD). The distribution widths were quantified by the Polydispersity Index (PdI). DLS measurements were carried out at 25°C before and after filtration (through acetate-cellulose Costar Spin-X Centrifuge Tube Filters, 0.22 µm pore size, Cole Parmer, USA) or centrifugation (18,000 × *g* for 15 min) of Qtracker®800 solutions. No filtration or centrifugation were used on the Qtracker®800 solutions employed for the *in vivo* and *in vitro* experiments.

Zeta potential measurements

Measurements were performed with a Zetasizer Nano ZS instrument (Malvern Instruments Ltd.). Qtracker®800 particles were dispersed at a final concentration of 75 nM in phosphate buffer, pH 7.4 and transferred to a disposable zeta cell. Measurements were carried out at 25°C after 120 s equilibration time, performing seven runs comprising 12 subruns each. The applied voltage was 100 V and the measured conductibility was 4.540 ± 0.334 mS cm^{-1}. All measurements passed technical quality criteria based on inspection of phase and frequency plots, and were reproducible after sample spinning at 18,000 × *g* for 15 min. Zeta potential was evaluated from electrophoretic mobility applying the Henry equation.

Animals & QD injection

Male Balb/c mice acquired from Harlan-Nossan (Udine, Italy) were adapted to the laboratory and

maintained on a 12-h inverted light/dark cycle, at 23 ± 1°C, with access to food and water *ad libitum*. Experiments started when animals were 6 weeks old and weighed 25 ± 5 g.

Experiments were approved by the University of Verona ethical committee. Animals (n = 10) were divided into two equal groups, one received injection of saline solution and the other of Qtracker®800, and both groups were sacrificed 3 h after injection.

Qtracker®800 solutions (or saline) were administered through a single injection (0.4 µM, 10 µl/g for each mouse) into the tail vein. Mice were then deeply anesthetized (zolazepam and tiletamine, ip. 20 mg/kg), and perfused transcardially with PBS followed by phosphate-buffered 4% paraformaldehyde. Cortical brain samples were collected to evaluate Qtracker®800 presence in the endothelium, based on transmission electron microscopy (TEM) and immunohistochemistry analysis.

According to the recommendation of the producer, the optimal time-interval for *in vivo* vasculature imaging with Qtracker®800 is 3 h post-injection [18]. Therefore, the 3-h time point is essential in understanding Qtracker®800 distribution into the cerebral bloodstream and if this time interval is sufficient for the nanoparticles to interact with the mouse brain vascular endothelium.

Transmission electron microscopy

Brain tissue samples were fixed in 2% glutaraldehyde in Sorensen buffer pH 7.4 for 2 h, postfixed in 1% osmium tetroxide in aqueous solution (2 h), dehydrated in graded concentrations of acetone and embedded in Epon-Araldite mixture (Electron microscopy Sciences, PA, USA). Ultrathin tissue sections (70 nm) were placed on Cu/Rh grids with Ultracut E (Reichert, Wien, Austria) and were observed using a Morgagni 268D microscope (Philips, The Netherlands).

For imaging the Qtracker®800 in solution, a droplet of nanoparticle solution was put on the grid (FCF-150-Cu, Electron Microscopy Science, PA, USA) and, after drying, the grid was imaged without any other processing.

Human umbilical vein endothelial cell cultures

HUVECs from seven healthy donors were individually harvested as previously described [28] and used between passages 2 and 5. The medium was refreshed every 2 days. At the beginning of each experiment, cells were harvested by trypsinization, using 0.05% trypsin (Sigma-Aldrich) and 0.537 mM EDTA in phosphate-buffered saline without calcium and magnesium (Seromed, Berlin, Germany). Cells were plated at a density of 2×10^4 cells/cm^2 onto 24-mm cover glasses for intracellular calcium imaging measurements.

Mouse brain endothelial cell cultures

Primary cultures of brain microvascular endothelial cells (BMVECs from Balb/c mice, passage 3–6; #PB-BALB-5023, PELOBiotech, Germany) were cultivated according to the producer's protocol. bEnd.3 (passage 22–30; #ATCC® CRL-2299™, VA, USA), a Balb/c mouse cell line, was grown in DMEM with Glutamax-I, 10% fetal bovine serum (Gibco, NY, USA), 100 U/ml penicillin, 100 µg/ml streptomycin, 5% CO_2 (37°C). Cells were plated at a density of 2×10^4 cells/cm^2 onto 24-mm cover glasses for intracellular calcium imaging measurements or 96-well plates for viability assays.

In-vitro Qtracker®800 studies

In order to apply Qtracker®800 *in vitro* in concentrations comparable to those used for the *in vivo* studies, we first estimated that the above-described injections yielded blood concentrations around 44-nM nanoparticles, based on a mouse whole blood volume of approximately 2 ml [29]. Taking into account this approximate value and the range of concentrations previously reported for *in vitro* studies using Qtracker®655 [30], we used between 10 and 40 nM Qtracker®800 in our *in vitro* experiments. To shed light on the Qtracker®800 direct action against brain microvascular endothelial cells, we performed calcium imaging and cell viability measurements on bEnd.3 cells and BMVECs.

Intracellular calcium imaging on endothelial cells

Fura-2 AM-based, Ca^{2+} imaging experiments on endothelial cells were performed as previously described [31]. Images were captured using a cooled CCD camera (Clara, Andor, Northern Ireland) in a setup including a monochromator Polychrome V (Till Photonics, Germany) coupled to an inverted microscope (Diaphot 200, Nikon, Japan), and were acquired on a computer using an image acquisition software (Live Acquisition, Till Photonics, Germany). Solutions were delivered on top of the endothelial cells through a 100-µm quartz perfusion head using an 8-channel valve pressurized perfusion system (ALA Scientific Instruments, NY, USA). Cells were incubated with Fura-2 AM (2.5 µM) and pluronic acid (F-127, 0.01%) for 45 min. After 15 min, the necessary time for Fura-2AM de-esterification, the cells were imaged. Before starting the nanoparticle flux, the cell monolayer was perfused with Ringer HEPES-buffered for 5 min. Cytosolic Ca^{2+} transients were elicited by the administration of 20 nM Qtracker®800 for 5 min followed, after a

Ringer HEPES-buffered wash-out period of 10 min, by the application of either ATP (30 µM, 20 s) for BMVECs and bEnd.3 cells, or histamine (10 µM, 20 s) for HUVECs. ATP and histamine are topical vasoactive substances that regulate brain capillary blood flow and vascular permeability [24,32], and were therefore used as positive controls for evoking intracellular calcium transients in endothelial cells. Cells that did not show a response to the positive control were excluded from subsequent analyses.

Endothelial cell viability by Trypan blue assay

Trypan blue assay was performed on bEnd.3 and BMVECs in control conditions and after 24-h treatment with Qtracker®800 (10, 20 and 40 nM). Cells were detached by trypsin, trypan blue was added (0.2%) and viable cells were counted (at least 150 cells). The viability was calculated relative to controls. Measurements were done in three replicates. Cells exposed to 3 mM H_2O_2 (1 h) were used as positive control.

Data analysis

Data analysis was performed using OriginPro 8 (OriginLab Corporation, MA, USA), Offline Acquisition software (Till Photonics, Germany) and Matlab (Mathworks, MA, USA).

Intracellular calcium changes were estimated from the ratio $R = I_{340\,nm}/I_{380\,nm}$ (I_{340} and I_{380} are the intensities measured at the emission wavelength of 510 nm when Fura-2 was excited at 340 and 380 nm, respectively). The ratio R was calculated in regions of interest (ROIs) covering each cell in the microscope field, after background subtraction.

R values were corrected by subtracting baseline signals averaged over the 5 min of perfusion prior to the application of nanoparticles. The resulting ΔR values were used for subsequent analyses. Only responses with an amplitude higher than three-times the SD of the background noise (measured before QDs administration) were considered.

In view of the lack of standard quantitative methods to describe calcium transients in the literature [26], we defined a set of parameters characterising the signal envelope (Figure 1). The onset and offset of the response were marked by the signal raising above and descending below a 5% threshold of the peak amplitude (ΔR_{max}). Response latency was the time from beginning of nanoparticle perfusion to response onset. Total response duration was the interval between response onset and offset. In order to differentiate between fast transients with sustained late responses and signals reaching a peak later in time, we computed a response asymmetry ratio (b/a), where a is the time from response onset to peak, and b is the time from response peak to offset. Total response area was the integral over response duration. Finally, we computed the maximum slope of the ascending transient (V_{max}). Pairwise correlations (along with Pearson and Spearman coefficients) among these parameters were computed with custom Matlab scripts. One-way ANOVAs followed by Fisher LSD *post hoc* tests were used to assess BMVEC and bEnd.3 endothelial cell viability, comparing cells treated with different concentrations of Qtracker®800 to untreated controls.

Results

Characterization of nanoparticles (size, hydrodynamic diameter & zeta-potential)

We measured the hydrodynamic diameter of Qtracker®800 by means of the DLS technique. DLS measurements were performed on QDs dissolved in saline solution or in Ringer HEPES-buffered solution.

For both saline and HEPES-buffered Ringer solutions, we found in the intensity distribution plots a major peak centered near the expected size of Qtracker®800 (Figure 2A & B), as well as a minor peak corresponding to larger components (for example, aggregates of nanoparticles). The DLS graphs in Figure 2 refer to 50 nM Qtracker®800, but note that the distribution did not significantly change for the analyzed range of nanoparticle concentrations (40–80 nM). A global polydispersity index (PdI) of approximately 0.35 was determined for both solutions. The major, lower diameter peak can be attributed to isolated Qtracker®800 particles. Given the wider scattering of larger particles, the relative populations of the species corresponding to the two peaks can be better appreciated after conversion of the data into a number distribution (dotted lines), which results in a single peak and confirms the prevalence of well-dispersed Qtracker®800 particles.

An attempt to remove the larger size contaminant by filtration was unsuccessful. On the other hand, centrifugation followed by DLS measurements on the supernatant resulted in very clean samples displaying a single peak in size distribution plots (Figure 2C &D). The monomodal distribution observed for these two preparations allowed us to perform a rigorous cumulant analysis and evaluate the harmonic intensity-averaged particle diameter (Z-average). The Z-average of Qtracker®800 was 36.56 ± 0.13 nm in Ringer HEPES-buffer (PdI = 0.180) and 35.80 ± 0.34 nm in saline solution (PdI = 0.151). The zeta potential value was -0.0124 ± 0.206 mV, indicating that Qtracker®800 particles are essentially neutral at pH 7.4. Qtracker®800 were also characterized by TEM (Figure 3A) and their cores, as visualized in suspension, were irregular in shape and their longest axis measured on average 8.27 ± 1.27 nm (SD).

Qtracker®800 accumulation in mouse brain microvascular endothelium

We then proceeded to evaluate the interaction of Qtracker®800 with the brain vascular endothelium in Balb/c mice upon nanoparticle injection. TEM analysis of mouse cortical brain sections indicated the presence of Qtracker®800 in the brain vascular endothelium 3 h after the intravenous injection, the time window recommended by the nanoparticle producer for vasculature imaging studies (Figure 3B & C). Nanoparticles can be detected in the cytoplasm, both concentrated within vesicle-like structures, and free in the cytosol. An in-depth histological characterization (sampling different brain regions and cellular compartments, different time-points or even different organs) of the of Qtracker®800 nanoparticle distribution is beyond the scope of the present study.

Qtracker®800 treatment does not lead to major cell death *in vitro*

Given the *in vivo* accumulation of Qtracker®800 in mouse brain endothelium demonstrated by TEM data, we have further verified, by *in vitro* tests, if nanoparticle administration modified endothelial cell viability. Viability slightly decreased as a function of nanoparticle concentration (BMVECs: $F(3,8) = 5.25$, $p < 0.05$; bEnd.3s: $F(3,8) = 5.37$, $p < 0.05$). Fisher *post hoc* tests confirmed that the reduction was statistically significant only for the highest nanoparticle concentration, when viability dropped to about 93% (Figure 4).

Qtracker®800 generate intracellular calcium transients in mouse brain endothelial cells & human umbilical vein endothelial cells

As *in vitro* endothelial cell viability tests revealed only small effects on cell survival of Qtracker®800 in the concentration ranges relevant for *in vivo* imaging studies (see section Materials & methods, '*In vitro* Qtracker®800 studies'), we explored the possibility of more subtle, functional nanoparticle-induced alterations of endothelial cells, by studying intracellular calcium fluctuations.

Acute (5 min) exposure to 20 nM Qtracker®800 generated cytosolic calcium transients in BMVECs (Figure 5A), bEnd.3 cells (Figure 5B) and HUVECs (Figure 5C & D). Based on the inclusion criteria described above, we found that 13.7% (52/380 cells) of BMVECs and 13.9% (57/410 cells) of bEnd.3 cells were responsive to Qtracker®800. Out of a total 1796 studied HUVECs, 189 (or 10.5%) responded to Qtracker®800. Interestingly, the fraction of responsive cells varied significantly between the seven donors (Figure 5D), suggesting the possibility that subjects may be either sensitive (20% or more of responsive cells) or nonsensitive (5% or less) to nanoparticles.

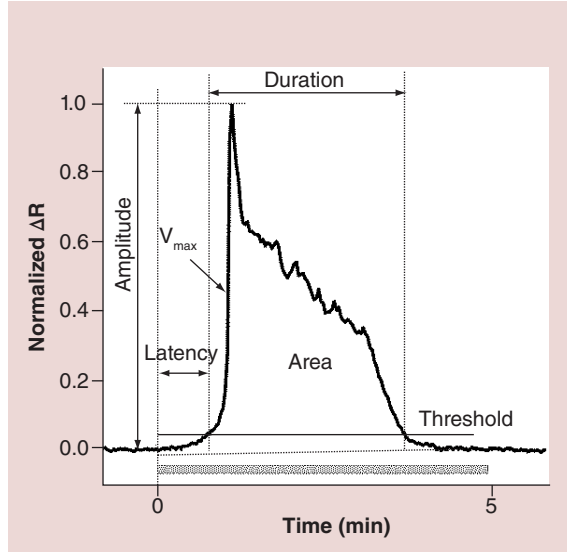

Figure 1. Relevant parameters in a calcium transient trace.

ΔR_{max} values induced by Qtracker®800 perfusion were on average a sizeable fraction of those induced in the positive control conditions. Namely, average ΔR_{max} values for BMVEC and bEnd.3 cells were about ⅓ and ½, respectively, of those produced by ATP administration; HUVEC cells had an average ΔR_{max} of about ⅔ of that induced by histamine administration (Figure 5E).

The quantitative analysis of calcium imaging recordings revealed a diversity of calcium transient profiles generated during the acute exposure of endothelial cells to the nanoparticle flux. The majority of observed calcium transients had a sharp onset, followed by a longer sustained response and decay (high asymmetry ratios). This pattern was substantially more marked in HUVECs than in mouse cells (Figures 5A–C & 6A).

In spite of certain commonalities, responses differed in several respects among cell types (Figure 6A). HUVEC transients showed the highest mean amplitude, area and duration (Figure 6A), in other words, they produced the strongest responses to nanoparticle administration. HUVEC transients were also highly asymmetrical (~three-times more than the mouse endothelial transients). Interestingly, the ΔR_{max} and V_{max} distributions were remarkably similar. Indeed, a strong and highly significant correlation between the two parameters was observed (Figure 6B, upper panels. See also Supplementary Figures 1–3, Supplementary Material, for a complete presentation of the correlations and distribution histograms). This suggests that a very rapid increase in the ascending phase of the transient tends to produce high peak amplitudes. Even more important is the fact that the slope of the linear regression was very similar between

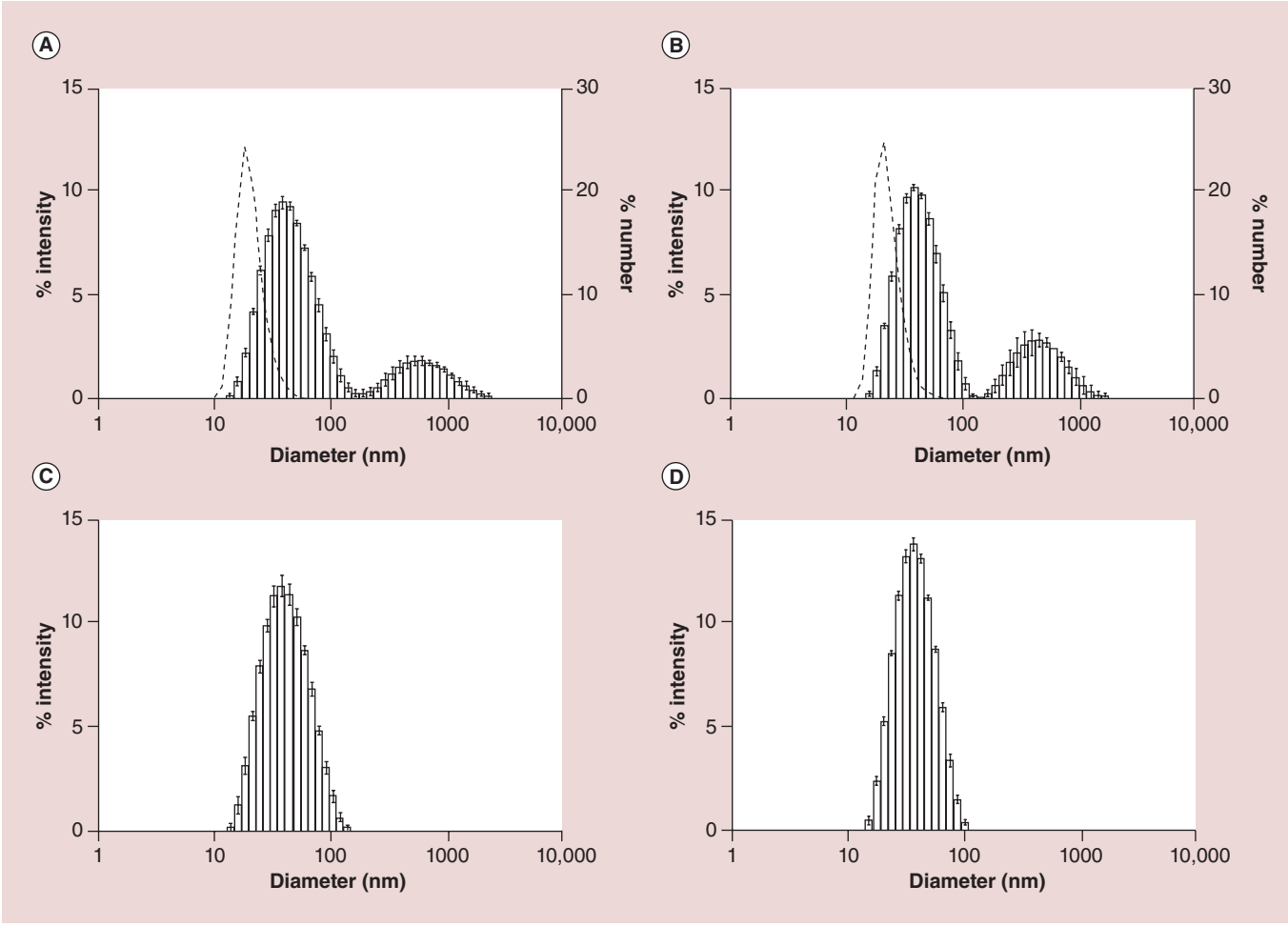

Figure 2. Distribution of Qtracker®800 particle sizes measured by dynamic light scattering. **(A)** Qtracker®800 in Ringer HEPES-buffer solution; **(B)** Qtracker®800 in saline solution; **(C)** same as **(A)** after centrifugation; **(D)** same as **(B)** after centrifugation. Histograms are size distribution by intensity plots (left y-axes). Error bars show the SD of three replicate measurements. Dotted curves in **(A & B)** correspond to number distribution plots (right y-axes) obtained by conversion from the underlying intensity distributions.

cell types. This suggests a common mechanism of calcium transient triggering, irrespective of endothelial types.

On the other hand, response latencies were similar across endothelial cell types, again suggesting a common triggering mechanism. Additionally, an interesting pattern was observed when plotting response latencies against V_{max} (Figure 6B, lower panels). The charts suggest that cells with relatively short latencies are characterized by a wide range of response transient velocities, while longer latencies were associated with relatively slower transients. In other words, delayed transients tended to be restricted to less steep ascending transients (smaller V_{max}) and consequently smaller amplitude.

Discussion

In this study, we report for the first time a functional interaction of Qtracker®800 with the brain vascular endothelium. In particular, we found that: QDs may be uptaken *in vivo* by brain endothelial cells; the interaction between QDs and endothelial cells results in the activation of free cytosolic calcium signaling in primary and immortalized brain endothelial cells, as well as in human umbilical vein endothelial cells; such activation does not appear to be related to cytotoxicity, resulting instead in interferences with normal calcium-mediated signal transduction pathways; HUVEC data indicate a high interindividual variability of QDs-cell interaction susceptibility.

Nontargeted PEGylated near-infrared emitting Qtracker®800 accumulate in brain vascular endothelium

Previous studies demonstrated the uptake by endothelial cells of different functionalized and/or targeted PEGylated quantum dots [33–35], but not of nontargeted Qtracker® Vascular labels. The latter nanopar-

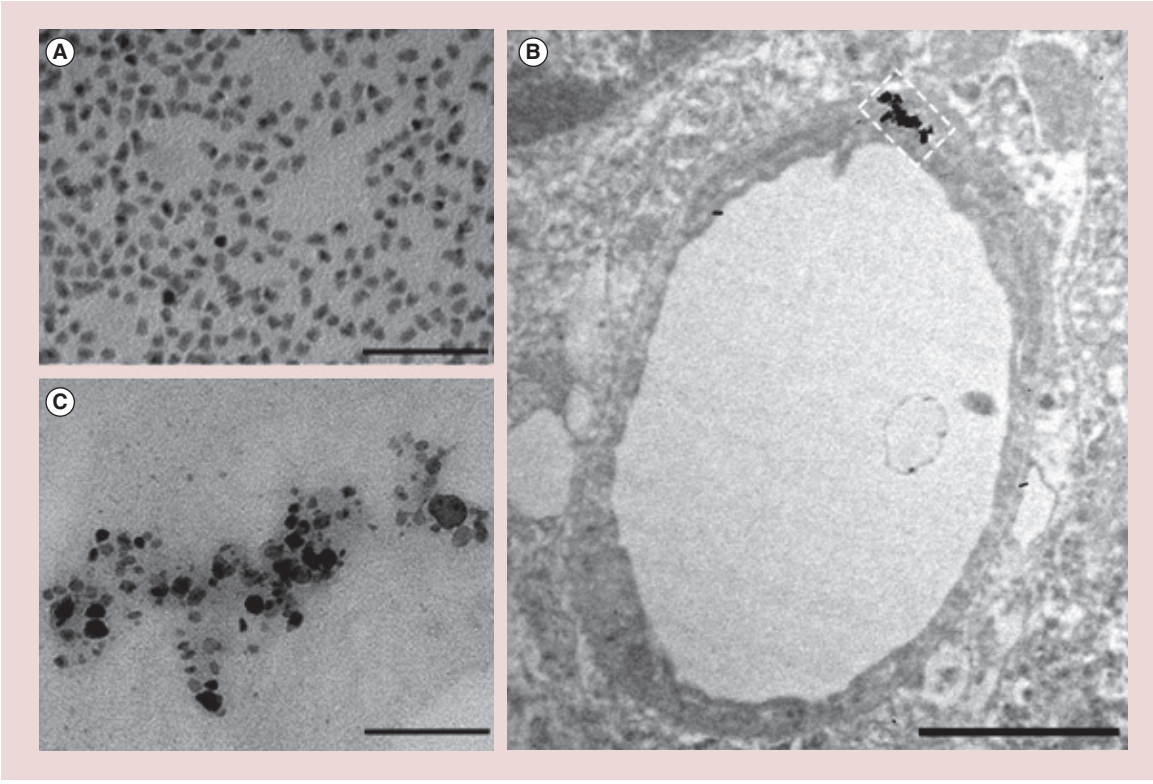

Figure 3. Transmission electron microscopy images on Qtracker®800 and their accumulation in Balb/c mouse brain endothelium. **(A)** Qtracker®800 in suspension; scale bar: 100 nm. **(B)** Qtracker®800 *in vivo* accumulation in brain vascular endothelium, 3 h after intravenous injection; scale bar: 1 μm. **(C)** Detailed image of nanoparticle accumulation in the endothelium; scale bar: 100 nm.

ticles can be uptaken in different cell types [30,36–38], but to our knowledge no reports are available for endothelial cells. Furthermore, uptake of Qtracker®800 has not been reported for any cell type.

Endocytosis, which is thought to be the main pathway for nanoparticle internalization [39,40], depends on nanoparticle size [41]. Specifically, endocytosis-mediated uptake of nanoparticles was found to be more efficient for hydrodynamic diameter values around 50 nm [42]. In this respect, although the optical qualities of Qtracker®800 make it suitable for deep vasculature imaging, their high hydrodynamic diameter (~35–36 nm based on our data) compared with the other dyes of the Qtracker® vascular label series (the second largest being the 26.6 nm Qtracker 705 [43]), makes them potentially more prone to endocytic internalization.

In *in vivo* or cell-culture experiments, the issue of nanoparticle fate is further complicated by the very complex media (blood, cell-culture medium) with which they interact. Very recent reports show the strong dependence of nanoparticle aggregation, particularly quantum dots, with respect to medium composition and coating structure [44,45]. Even in a simpler solution, bovine serum albumin in PBS, the hydro-

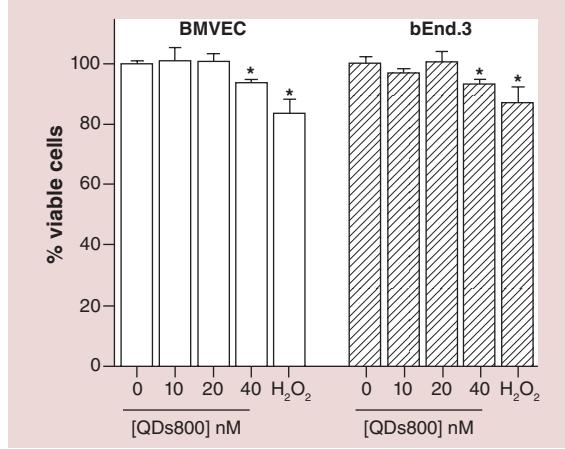

Figure 4. Viability of brain microvascular endothelial cells upon 24 h *in vitro* exposure to Qtracker®800. Percentage of viable cells (means ± standard deviation) obtained by Trypan blue assay on brain microvascular endothelial cells and bEnd.3 cells exposed for 24 h to 0, 10, 20 and 40 nM Qtracker®800 and 3 mM H_2O_2 (positive control). Statistically significant differences ($p < 0.05$) from the control (0 nM) conditions are indicated by an asterisk (*).
bEnd.3: Brain endothelial cell line derived from mice cerebral cortex; BMVEC: Brain microvascular endothelial cells from Balb/c mice in primary culture; QD: Quantum dot.

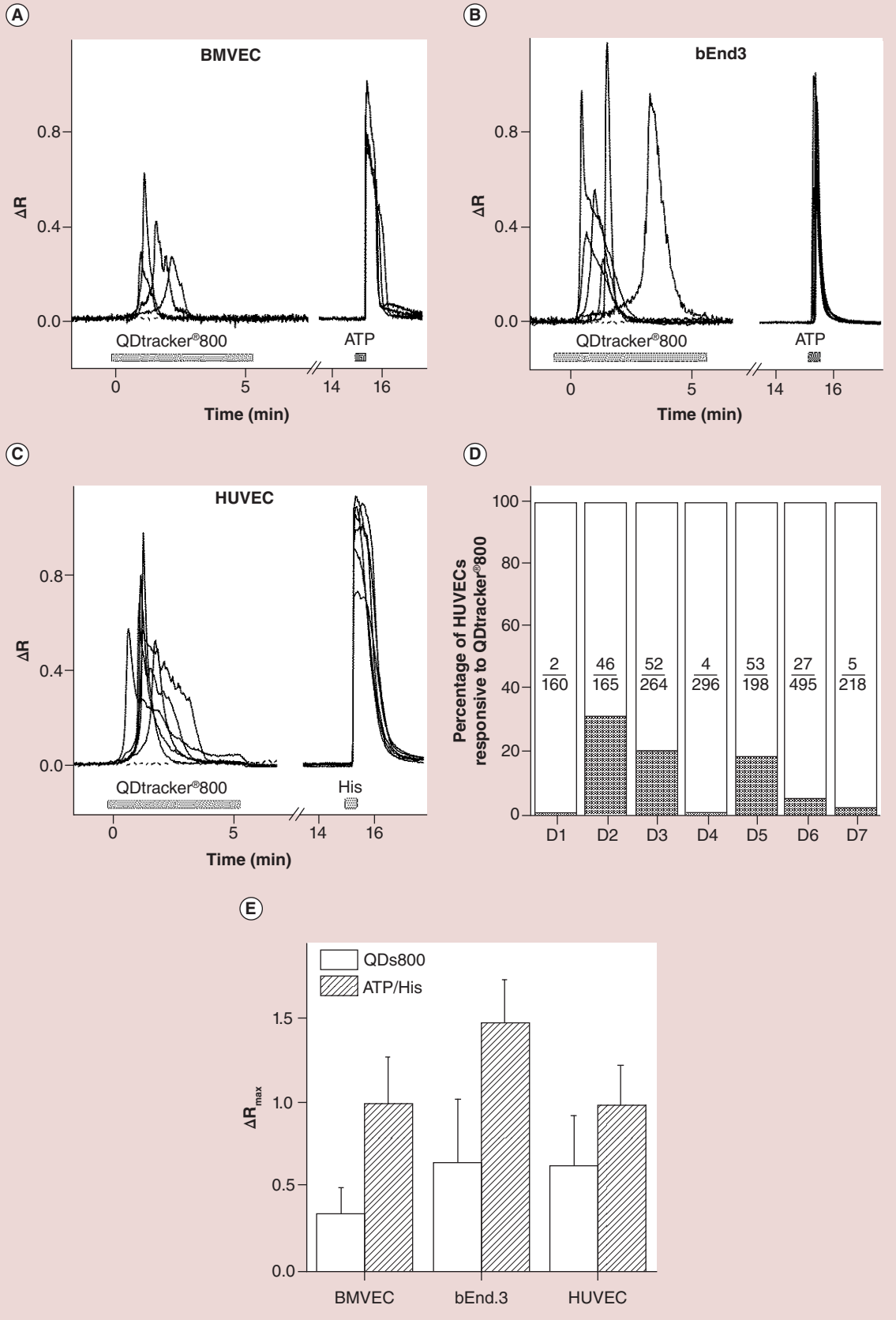
A
BMVEC
ΔR
0.8
0.4
0.0
QDtracker®800
ATP
0
5
14
16
Time (min)
B
bEnd3
ΔR
0.8
0.4
0.0
QDtracker®800
ATP
0
5
14
16
Time (min)
C
HUVEC
ΔR
0.8
0.4
0.0
QDtracker®800
His
0
5
14
16
Time (min)
D
Percentage of HUVECs responsive to QDtracker®800
100
80
60
40
20
0
2/160
46/165
52/264
4/296
53/198
27/495
5/218
D1
D2
D3
D4
D5
D6
D7
E
QDs800
ATP/His
ΔR max
1.5
1.0
0.5
0.0
BMVEC
bEnd.3
HUVEC

Figure 5. Qtracker®800 evoked $(Ca^{2+})_i$ transients in mouse and human endothelial cells (see facing page).
Representative traces of ΔR over time for **(A)** brain microvascular endothelial cells; **(B)** bEnd3, and **(C)** HUVECs. An endogenous control response was evoked by ATP (30 μM) in **(A & B)**, and by histamine (10 μM) in **(C)**. **(D)** HUVECs' sensitivity to Qtracker®800 exposure, where responsive cells are considered those able to generate intracellular calcium transients upon brief exposure (5 min) to Qtracker®800. Percentage of responsive (gray) and nonresponsive (white) endothelial cells from different donors. The number of Qtracker®800-responsive cells are plotted against the total number of tested cells in separate columns for each donor (D1–D7). The percentages of responsive cells for each donor are: D1: 1.25%; D2: 27.87%; D3: 19.69%; D4: 1.35%; D5: 26.76%; D6: 5.45%; D7: 2.29%. **(E)** ΔR_{max} for BMVEC, bEnd.3 and HUVEC in response to Qtracker®800 and to ATP or His, respectively. bEnd.3: Brain endothelial cell line derived from mice cerebral cortex; BMVEC: Brain microvascular endothelial cells from Balb/c mice in primary culture; D: Donor; His: Histamine; HUVEC: Human umbilical vein endothelial cell; QD: Quantum dot.

dynamic diameter of Qtracker®800, as measured by DLS, increased with albumin concentrations, becoming more than double at protein concentrations equivalent to those present in the mouse blood serum [46]. Blood fibrinogen was also proven to strongly bind Qtracker®800 [47]. In this context, it is very difficult to further speculate about the mechanism by which Qtracker®800 particles are uptaken into the cells.

A vascular label such as the Qtracker® nanoparticles is expected to be inert with respect to the physiology of the target system. Our study, however, shows that nontargeted, near-infrared emitting Qtracker®800 are captured by the brain vascular endothelium in the first 3 h upon vein injection, which raises important concerns, including the possibility that such uptake (and interaction more in general) may lead to alteration of endothelial cell functionality.

Qtracker®800 alters 'normal' calcium signaling in brain endothelial cells

It was previously shown that acute exposure (5–30 min) to non-PEGylated or functionalized QDs elicits *in vitro* cytosolic calcium increases in different excitable and nonexcitable cells [48–51]. Our study points out that nanoparticle PEG-ylation, at least in the case of Qtracker®800, does not prevent functional consequences on the vascular endothelium, as revealed by the occurrence of calcium transients during the 5-min exposure.

The vascular endothelium has mechanosensitive properties, as part of the adaptation to the permanent shear stress exerted by the bloodstream. Endothelial cells may react to mechanical stimuli through a variety of mechanisms, such as transient receptor potential channels, ATP-operated cation channels, GTP-binding protein coupled receptors and adhesion molecules [52]. In turn, a variety of downstream intracellular signaling pathways are activated, the majority involving either calcium release from internal stores, the intake of extracellular calcium or both [51,53]. The strong positive correlation between calcium release amplitude (ΔR_{max}) and steepness (V_{max}) shown in the present study has similarities with the previously reported amplitude-dependent calcium release in response to local mechanical stimuli [54] and might imply that Qtracker®800 act as a mechanical trigger for the calcium-induced transients.

The wide range of calcium event latencies we have observed, and the fact that only a subset of cells were activated, lead to the following speculation. Some cells are triggered by a probabilistic, direct interaction with the nanoparticles (possibly of mechanical nature) while neighboring cells are indirectly recruited in a wave of calcium events through intercellular communication mechanisms, as previously described in other endothelial cell types [55]. In this view, while fast and steep transients could be the result of direct nanoparticle-to-cell interactions, slower and shallower transients could be related to indirect activations.

Qtracker®800 might activate different components of the neurovascular unit

It has already been stated that brain microvascular endothelium is a major component of the neurovascular unit, playing essential roles in physiological and pathological neuronal-activation states [11,56,57]. The spatio-temporal Ca^{2+} dynamics contribute to many physiological properties of the vascular intima [26]; asynchronous and synchronous Ca^{2+} waves control vascular tone [58]. Local changes at the level of vascular endothelium (e.g., leukocyte-endothelial adhesion, leukocyte rolling) can translate into alterations of neuronal excitability [11]. In this general context, the Qtracker®800-induced intracellular endothelial Ca^{2+} transient activation shown by our results deserves attention in nanomedicine, and might imply not only localised endothelial Ca^{2+} events but also the initiation of a complex signaling pathway involving multiple components of the neurovascular unit. Previous studies have highlighted the action of nanoparticles on different components of the neurovascular unit, by demonstrating that Qtracker®705: accumulate *in vitro* in primary cortical cultures; activates astrocytes after microinjection in brain cortex [36]. Furthermore, large silica (NH_2) PEGylated nanoparticles *in vitro* are uptaken into bEnd.3 cells and, *in vivo*, are transported across the blood-brain barrier in Balb/c mice [23].

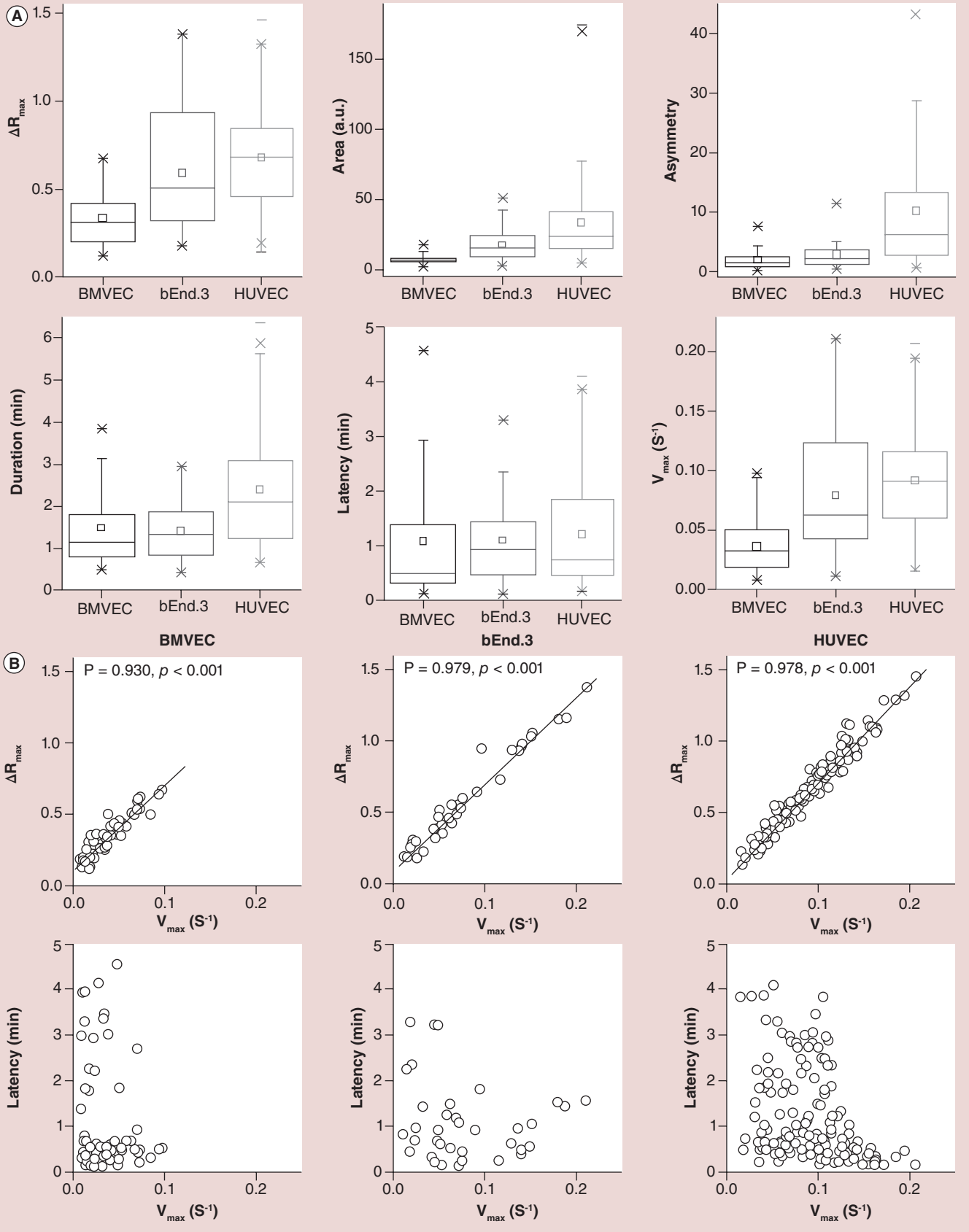
A
ΔRmax
Area (a.u.)
Asymmetry
Duration (min)
Latency (min)
Vmax (S-1)
BMVEC
bEnd.3
HUVEC
B
P = 0.930, p < 0.001
P = 0.979, p < 0.001
P = 0.978, p < 0.001
Vmax (S-1)
Latency (min)

Figure 6. Analysis of the parameters in Qtracker®800-induced calcium transients (see facing page). (A) Distributions of each of the six calcium transient parameters (y-axis label) defined in the 'Materials & methods' section. The boxplots show the median, 25% and 75% percentiles. In addition, the mean (□), 1% and 99% percentiles (×), and the minimum and maximum data points (-) are reported. **(B)** Correlations between selected parameter pairs for each cell type (the linear fit with Pearson coefficient – P, and the confidence level – p – are presented for the upper panels). See Supplementary Material for the complete pairwise correlation matrices. BMVEC: Brain microvascular endothelial cells from Balb/c mice in primary culture; HUVEC: Human umbilical vein endothelial cell; V_{max}: Maximum slope of the ascending calcium transient.

Based on our data, we wonder whether Qtracker®800-induced alteration of 'normal' calcium signaling in endothelial cells may bias the interpretation of results in studies of brain vascular function where nanoparticles are used as labels.

How suitable are Qtracker®800 for translational studies?

Our results indicate that the nanoparticle-induced endothelial activation is not specific to mouse brain vessels, but it extends at least to a different species (human) and a different endothelial cell localization (umbilical vein). A further generalization of the observation will require *ad hoc* studies on endothelial cells derived from other species and organs.

A key result in our study is the striking difference in HUVEC sensitivity to Qtracker®800 from one donor to another (almost an all-or-none effect). Our data agree with previously reported donor-dependent variability of HUVECs exposed to laminar shear stress [59], and might have implications for the use of near-infrared-emitting quantum dots in clinical vascular imaging applications.

Whether a similar donor-dependent variability of responses in HUVECs exists also in rodents is not easy to establish, since *in vitro* studies make use of sample pooling between several subjects (approximately ten mice for a single culture [60]). But this is a relevant issue, because if on one hand the mean number of activated cells in mice and in humans are comparable (13.7 vs 10.5%) establishing potential effects based on such averages might underestimate the effects on the individuals more prone to QD-induced activations.

Conclusion & future perspective

Our study partly fills the knowledge gap regarding the interaction of near-infrared-emitting Qtracker®800 nanoparticles with biological systems, in particular the brain vascular endothelium. Both *in vitro* and *in vivo* data indicate the accumulation of QDs in the vascular endothelium as well as functional effects revealed by intracellular calcium changes in a subset of cells. In addition, we observed substantial interindividual differences in HUVEC activation. Altogether, the findings raise two types of concern: in studies of vascular function in living animals, the use of QD-based labeling might bias the results in difficult-to-detect ways; in view of possible clinical applications, the between-subject variability in susceptibility may complicate safety assessments.

Undoubtedly, brain vasculature imaging techniques can greatly benefit from the use of nanoparticle labels. On the other hand, as we have shown, such labels may be internalized by and functionally interact with blood vessel endothelia, which raises obvious safety concerns. It is quite possible that the effects uncovered represent the tip of an iceberg, and that further studies are necessary to better characterize the full extent and consequences of the activations. Ideally, the development of novel labels should be focused on reducing or eliminating their interactions with biological tissues. Considering the vast potential of these nanoparticles for brain vasculature imaging, we hope that further chemical engineering will optimize their biostability, biocompatibility and efficient clearance profile.

Supplementary data

To view the supplementary data that accompany this paper, please visit the journal website at: www.futuremedicine.com/doi/full/10.2217/NNM.15.120

Acknowledgements

The authors are grateful to S Becchi and E Nicolato for their precious help in the early steps of the research. The authors acknowledge M Ameloot (University of Haaselt, Belgium) for granting the use of the microscope oil objective 40× for calcium imaging measurements. The authors acknowledge S Roffler from the Institute of Biomedical Sciences, Academia Sinica, Taiwan for kindly gifting us the AGP4 antibodies.

Financial & competing interests disclosure

This work was in part supported by the Verona Nanomedicine Initiative – WP4, financed by Fondazione Cariverona. BM Radu is the holder of a PhD fellowship financed by the Italian Ministry of Education, University and Research (MIUR). The authors have no other relevant affiliations or financial involvement with any organization or entity with a financial interest in or financial conflict with the subject matter or materials discussed in the manuscript apart from those disclosed.

No writing assistance was utilized in the production of this manuscript.

Ethical conduct of research

The authors state that they have obtained University of Verona review board approval. In addition, for investigations involving human subjects, informed consensus has been obtained from the participants involved and they have followed the principles outlined in the Declaration of Helsinki for all human or animal experimental investigations. In addition, for investigations involving human subjects, informed consent has been obtained from the participants involved.

Executive summary

Aim

- To assess the possible interaction of Qtracker® 800 Vascular labels (Qtracker®800), a powerful nanotechnology tool for biomedical vasculature imaging, with mouse and human endothelium.

Results

- Transmission electron microscopy showed Qtracker®800 accumulation in mouse brain microvascular endothelium 3 h after their administration.
- Mouse brain endothelial cells, both in primary and immortalized cultures, are Qtracker®800-sensitive; 14% of cells generate intracellular calcium transients during acute 5-min exposures.
- Human umbilical vein endothelial cells in primary culture derived from different donors present substantial variability in transient calcium responses (0 ÷ 30%) when acutely exposed to Qtracker®800.
- The chronic *in vitro* exposure to Qtracker®800 for 24 h did not reveal major changes in endothelial cell viability.

Conclusion & future perspective

- We demonstrated a direct action of Qtracker®800 on the vascular endothelium in the first 3 h after administration, thus overlapping the time window recommended for vasculature imaging studies with these fluorescent nanoparticles.
- Keeping in mind the enormous potential of Qtracker®800 deep-tissue penetration in biomedical applications, better manufacturing solutions to diminish/eliminate endothelium actions should be found.

References

Papers of special note have been highlighted as:
• of interest; •• of considerable interest

1 Kim BY, Rutka JT, Chan WC. Nanomedicine. *N. Engl. J. Med.* 363(25), 2434–2443 (2010).

2 Clift MJ, Stone V. Quantum dots: an insight and perspective of their biological interaction and how this relates to their relevance for clinical use. *Theranostics* 2(7), 668–680 (2012).

• **Describes the current knowledge on quantum dot (QD) interactions with biological systems and their clinical relevance.**

3 Burns AA, Vider J, Ow H *et al.* Fluorescent silica nanoparticles with efficient urinary excretion for nanomedicine. *Nano Lett.* 9(1), 442–448 (2009).

4 Benezra M, Penate-Medina O, Zanzonico PB *et al.* Multimodal silica nanoparticles are effective cancer-targeted probes in a model of human melanoma. *J. Clin. Invest.* 121(7), 2768–2780 (2011).

5 Bradbury MS, Phillips E, Montero PH *et al.* Clinically-translated silica nanoparticles as dual-modality cancer-targeted probes for image-guided surgery and interventions. *Integr. Biol. (Camb.)* 5(1), 74–86 (2013).

•• **The first US FDA-approved, clinically translated fluorescent silica nanoparticles (~6–7 nm diameter) for use with PET and optical imaging in the detection and localization of sentinel lymph node metastases.**

6 Ding D, Goh CC, Feng G *et al.* Ultrabright organic dots with aggregation-induced emission characteristics for real-time two-photon intravital vasculature imaging. *Adv. Mater.* 25(42), 6083–6088 (2013).

7 Jaruszewski KM, Curran GL, Swaminathan SK *et al.* Multimodal nanoprobes to target cerebrovascular amyloid in Alzheimer's disease brain. *Biomaterials* 35(6), 1967–1976 (2014).

8 Li C, Zhang Y, Wang M *et al. In vivo* real-time visualization of tissue blood flow and angiogenesis using Ag2S quantum dots in the NIR-II window. *Biomaterials* 35(1), 393–400 (2014).

9 Keunen O, Taxt T, Grüner R *et al.* Multimodal imaging of gliomas in the context of evolving cellular and molecular therapies. *Adv. Drug Deliv. Rev.* 76, 98–115 (2014).

10 Radu BM, Radu M. Recent preclinical and clinical technological advances suitable to unravel the blood brain barrier characteristics in physiological and pathological neurological states. *EC Neurol.* 1(2), 22–27 (2015).

11 Fabene PF, Navarro Mora G, Martinello M *et al.* A role for leukocyte-endothelial adhesion mechanisms in epilepsy. *Nat. Med.* 14(12), 1377–1383 (2008).

12 Burrell K, Agnihotri S, Leung M, Dacosta R, Hill R, Zadeh G. A novel high-resolution *in vivo* imaging technique to study the dynamic response of intracranial structures to tumor growth and therapeutics. *J. Vis. Exp.* 76, e50363 (2013).

13 Hyun H, Lee K, Min KH *et al.* Ischemic brain imaging using fluorescent gold nanoprobes sensitive to reactive oxygen species. *J. Control. Release* 170(3), 352–357 (2013).

14 Zhu Y, Hong H, Xu ZP, Li Z, Cai W. Quantum dot-based nanoprobes for *in vivo* targeted imaging. *Curr. Mol. Med.* 13(10), 1549–1567 (2013).

15 Medintz IL, Uyeda HT, Goldman ER, Mattoussi H. Quantum dot bioconjugates for imaging, labelling and sensing. *Nat. Mater.* 4(6), 435–446 (2005).

16 Michalet X, Pinaud FF, Bentolila LA *et al.* Quantum dots for live cells, *in vivo* imaging, and diagnostics. *Science* 307(5709), 538–544 (2005).

• **Describes the current approaches for the synthesis, solubilization and functionalization of QDs and their applications in cell and animal biology.**

17 Stylianou P, Skourides PA. Imaging morphogenesis, in xenopus with quantum dot nanocrystals. *Mech. Dev.* 126(10), 828–841 (2009).

18 Qtracker®800 Vascular Labels. www.lifetechnologies.com

19 Mayes P, Dicker D, Liu Y, El-Deiry W. Noninvasive vascular imaging in fluorescent tumors using multispectral unmixing. *Biotechniques* 45(4), 459–464 (2008).

• **Reports Qtracker®800 use for imaging tumor vasculature with multispectral unmixing.**

20 Lo Celso C, Lin CP, Scadden DT. *In vivo* imaging of transplanted hematopoietic stem and progenitor cells in mouse calvarium bone marrow. *Nat. Protoc.* 6(1), 1–14 (2011).

21 Bentzen EL, Tomlinson ID, Mason J *et al.* Surface modification to reduce nonspecific binding of quantum dots in live cell assays. *Bioconjug. Chem.* 16(6), 1488–1494 (2005).

22 Kelf TA, Sreenivasan VK, Sun J, Kim EJ, Goldys EM, Zvyagin AV. Non-specific cellular uptake of surface-functionalized quantum dots. *Nanotechnology* 21(28), 285105 (2010).

• **Demonstrates the reduction of QDs' nonspecific cellular uptake by PEG coating.**

23 Liu D, Lin B, Shao W, Zhu Z, Ji T, Yang C. *In vitro* and *in vivo* studies on the transport of PEGylated silica nanoparticles across the blood-brain barrier. *ACS Appl. Mater. Interfaces* 6(3), 2131–2136 (2014).

24 Itoh Y, Suzuki N. Control of brain capillary blood flow. *J. Cereb. Blood Flow Metab.* 32(7), 1167–1176 (2012).

25 Moccia F, Tanzi F, Munaron L. Endothelial remodelling and intracellular calcium machinery. *Curr. Mol. Med.* 14(4), 457–480 (2014).

26 Taylor MS, Francis M. Decoding dynamic Ca^{2+} signaling in the vascular endothelium. *Front. Physiol.* 5, 447 (2014).

•• **Correlates the endothelial Ca^{2+} dynamics with vasoregulatory mechanisms.**

27 Ceccon A, D'Onofrio M, Zanzoni S *et al.* NMR investigation of the equilibrium partitioning of a water-soluble bile salt protein carrier to phospholipid vesicles. *Proteins* 81(10), 1776–1791 (2013).

28 Fratta Pasini A, Albiero A, Stranieri C *et al.* Serum oxidative stress-induced repression of Nrf2 and GSH depletion: a mechanism potentially involved in endothelial dysfunction of young smokers. *PLoS ONE* 7(1), e30291 (2012).

29 Endo K, Kito N, Fukushima Y, Weng H, Iwai N. A novel biomarker for acute kidney injury using TaqMan-based unmethylated DNA-specific polymerase chain reaction. *Biomed. Res.* 35(3), 207–213 (2014).

30 Zhang LW, Monteiro-Riviere NA. Mechanisms of quantum dot nanoparticle cellular uptake. *Toxicol. Sci.* 110(1), 138–155 (2009).

31 Radu BM, Dumitrescu DI, Mustaciosu CC, Radu M. Dual effect of methylglyoxal on the intracellular Ca^{2+} signaling and neurite outgrowth in mouse sensory neurons. *Cell. Mol. Neurobiol.* 32(6), 1047–1057 (2012).

32 Akdis CA, Simons FER. Histamine receptors are hot in immunopharmacology. *Eur. J. Pharmacol.* 533(1–3), 69–76 (2006).

33 Koole R, van Schooneveld MM, Hilhorst J *et al.* Paramagnetic lipid-coated silica nanoparticles with a fluorescent quantum dot core: a new contrast agent platform for multimodality imaging. *Bioconjug. Chem.* 19(12), 2471–2479 (2008).

34 Pollinger K, Hennig R, Ohlmann A *et al.* Ligand-functionalized nanoparticles target endothelial cells in retinal capillaries after systemic application. *Proc. Natl Acad. Sci. USA* 110(15), 6115–6120 (2013).

35 Chen Y, Molnár M, Li L *et al.* Characterization of VCAM-1-binding peptide-functionalized quantum dots for molecular imaging of inflamed endothelium. *PLoS ONE* 8(12), e83805 (2013).

36 Maysinger D, Behrendt M, Lalancette-Hébert M, Kriz J. Real-time imaging of astrocyte response to quantum dots: *in vivo* screening model system for biocompatibility of nanoparticles. *Nano Lett.* 7(8), 2513–2520 (2007).

37 Ryman-Rasmussen JP, Riviere JE, Monteiro-Riviere NA. Surface coatings determine cytotoxicity and irritation potential of quantum dot nanoparticles in epidermal keratinocytes. *J. Invest. Dermatol.* 127(1), 143–153 (2007).

38 Xiao Y, Forry SP, Gao X, Holbrook RD, Telford WG, Tona A. Dynamics and mechanisms of quantum dot nanoparticle cellular uptake. *J. Nanobiotechnol.* 8, 13 (2010).

39 Damalakiene L, Karabanovas V, Bagdonas S, Valius M, Rotomskis R. Intracellular distribution of nontargeted quantum dots after natural uptake and microinjection. *Int. J. Nanomedicine* 8, 555–568 (2013).

40 Kou L, Sun J, Zhai Y, He Z. The endocytosis and intracellular fate of nanomedicines: implication for rational design. *Asian J. Pharmac. Sci.* 8(1), 1–10 (2013).

41 Shang L, Nienhaus K, Nienhaus GU. Engineered nanoparticles interacting with cells: size matters. *J. Nanobiotechnol.* 12, 5 (2014).

42 Osaki F, Kanamori T, Sando S, Sera T, Aoyama Y. A quantum dot conjugated sugar ball and its cellular uptake. On the size effects of endocytosis in the subviral region. *J. Am. Chem. Soc.* 126(21), 6520–6521 (2004).

43 Ho CC, Chang H, Tsai HT *et al.* Quantum dot 705, a cadmium-based nanoparticle, induces persistent inflammation and granuloma formation in the mouse lung. *Nanotoxicology* 7(1), 105–115 (2013).

44 Moquin A, Neibert KD, Maysinger D *et al.* Quantum dot agglomerates in biological media and their characterization by asymmetrical flow field-flow fractionation. *Eur. J. Pharm. Biopharm.* 89, 290–299, (2015).

45 Balog S, Rodriguez-Lorenzo L, Monnier CA *et al.* Characterizing nanoparticles in complex biological media and physiological fluids with depolarized dynamic light scattering. *Nanoscale* 7, 5991–5997 (2015).

46 Rampazzo E, Boschi F, Bonacchi S *et al.* Multicolor core/shell silica nanoparticles for *in vivo* and *ex vivo* imaging. *Nanoscale* 4(3), 824–830 (2012).

47 Pozzi-Mucelli S, Boschi F, Calderan L *et al.* Quantum Dots: Proteomics characterization of the impact on biological systems. *J. Phys. Conference Series* 170, 012021 (2009).

48 Tang M, Xing T, Zeng J *et al.* Unmodified CdSe quantum dots induce elevation of cytoplasmic calcium levels and impairment of functional properties of sodium channels in rat primary cultured hippocampal neurons. *Environ. Health Perspect.* 116(7), 915–922 (2008).

49 Tang M, Wang M, Xing T, Zeng J, Wang H, Ruan DY. Mechanisms of unmodified CdSe quantum dot-induced elevation of cytoplasmic calcium levels in primary cultures of rat hippocampal neurons. *Biomaterials* 29(33), 4383–4391 (2008).

50 Clift MJ, Boyles MS, Brown DM, Stone V. An investigation into the potential for different surface-coated quantum dots to cause oxidative stress and affect macrophage cell signalling *in vitro*. *Nanotoxicology* 4(2), 139–149 (2010).

51 Miragoli M, Novak P, Ruenraroengsak P *et al.* Functional interaction between charged nanoparticles and cardiac tissue: a new paradigm for cardiac arrhythmia? *Nanomedicine (Lond.)* 8(5), 725–737 (2013).

52 Ando J, Yamamoto K. Flow detection and calcium signalling in vascular endothelial cells. *Cardiovasc. Res.* 99(2), 260–268 (2013).

53 Tran QK, Ohashi K, Watanabe H. Calcium signalling in endothelial cells. *Cardiovasc. Res.* 48(1), 13–22 (2000).

54 Yamamoto K, Korenaga R, Ohura N, Sokabe T, Kamiya A, Ando J. Role of P2X4 purinoceptors in endothelial Ca^{2+} response to shear stress. *Ann. Biomed. Eng.* 28(Suppl. 1), S68 (2000).

55 Long J, Junkin M, Wong PK, Hoying J, Deymier P. Calcium wave propagation in networks of endothelial cells: model-based theoretical and experimental study. *PLoS Comput. Biol.* 8(12), e1002847 (2012).

56 Bertini G, Bramanti P, Constantin G *et al.* New players in the neurovascular unit: insights from experimental and clinical epilepsy. *Neurochem. Int.* 63(7), 652–659 (2013).

57 Radu BM, Bramanti P, Osculati F *et al.* Neurovascular unit in chronic pain. *Mediators Inflamm.* 2013, 648268 (2013).

58 Mufti RE, Brett SE, Tran CH *et al.* Intravascular pressure augments cerebral arterial constriction by inducing voltage-insensitive Ca^{2+} waves. *J. Physiol.* 588(Pt 20), 3983–4005 (2010).

59 Feairheller DL, Park JY, Rizzo V, Kim B, Brown MD. Racial differences in the responses to shear stress in human umbilical vein endothelial cells. *Vasc. Health Risk Manag.* 7, 425–431 (2011).

60 Ruck T, Bittner S, Epping L, Herrmann AM, Meuth SG. Isolation of primary murine brain microvascular endothelial cells. *J. Vis. Exp.* 93, e52204 (2014).